ELECTROCHEMICAL STUDY OF LITHIUM ION CELLS USING LIMN2O4 AS THE CATHODE AND CARBON NANOTUBES AS THE ANODE FOR DIFFERENT BINDER COMBINATIONS.

J. Mindiola[a], Y. F. Balladores[b]*, E. V. Plaza[c,d], J. E. Arévalo-Fester[e,f], R. Atencio[b,c], L. Corredor[g]

a) Universidad del Zulia, Facultad de Ciencias, 4011, Maracaibo, Venezuela.
b) Laboratorio de Materiales para Tecnologías Emergentes (LaMTE). Centro de Investigación y Tecnología de Materiales, Instituto Venezolano de Investigaciones Científicas (IVIC), 4011, Maracaibo, Venezuela.
c) Facultad de Ciencias Naturales y Matemáticas (FCNM), Escuela Superior Politécnica del Litoral, (ESPOL), Polytechnic University, 09015863, Guayaquil, Ecuador.
d) Laboratorio de Física de Fluidos y Plasma, Centro de Física, Instituto Venezolano de Investigaciones Científicas (IVIC), 1020-A, Altos de Pipe, Venezuela.
e) Unidad de Caracterización y Estructura de Materiales (UCEM). Instituto Zuliano de Investigaciones Tecnológicas (INZIT), 4001, Maracaibo, Venezuela.
f) Laboratorio de Síntesis y Caracterización de Nuevos Materiales (LSCNM), Instituto Venezolano de Investigaciones Científicas (IVIC), 1020-A, Altos de Pipe, Venezuela.
g) School of Physical Sciences and nanotechnology, Yachay Tech University, 100119-Urcuqui, Ecuador.

*Corresponding author, e-mail: *yanpiero@gmail.com*

ABSTRACT
Lithium-ion batteries have been widely used as a key alternative in the advancement of new energy generation and storage technologies. However, some of their features can still be improved. Nanostructured electrode materials are at the forefront of research in the field of energy storage, showing superior performances, higher energy, power densities, and a more significant number of charge-discharge cycles. In this work, electrochemical reversibility studies were carried out through the cyclic voltammetry technique applying the Nicholson and Shain criteria in a cell constructed from an anode of multi-walled carbon nanotubes (MWCNT) and lithium tetraoxomanganate(VI) (LiMn$_2$O$_4$) as the cathode, using lithium tetrafluoroborate (LiBF$_4$) as support electrolyte dissolved in propylene carbonate and an Ag/AgCl reference electrode. The products were also characterized by Scanning Electron Microscopy (SEM), Thermogravimetric Analysis (TGA), and X-ray Diffraction (XRD) analysis. Combinations of binders were used in the composites to improve the electrical conductivity in the electrodes, the mechanical properties, and the reversibility process. The electrochemical characterization reported the existence of a pair of characteristic anodic and cathodic peaks associated with the intercalation/deintercalation process of lithium ions at the electrode/electrolyte interface, expected behavior in Li-ion cells. Results showed that combinations of 70% LiMn$_2$O$_4$/25% Carbon (C)/5% polytetrafluoroethylene (PTFE) for the cathode material and 90% MWCNT/10% PTFE at the anode presented optimal results both for the intercalation and deintercalation of lithium, as well as for the adherence of the composite.

Keywords: Li-ion cells; binder; LiMn$_2$O$_4$; voltammetry; carbon nanotubes.

Estudio electroquímico de celdas de ion litio usando como cátodo LiMn$_2$O$_4$ y ánodo de nanotubos de carbono para diferentes combinaciones de aglomerante.

RESUMEN
Las baterías de ion de litio se han utilizado ampliamente como una alternativa clave en el avance de nuevas tecnologías de generación y almacenamiento de energía, sin embargo, algunas de sus características pueden aún ser mejoradas. Los electrodos nanoestructurados están a la vanguardia de la investigación sobre el almacenamiento de energía, mostrando rendimientos superiores, mayores densidades de energía, potencia y un número mayor de ciclos. En este trabajo se realizaron estudios de reversibilidad electroquímica empleando voltametría cíclica aplicando los criterios de Nicholson y Shain en una celda construida a partir de un ánodo de nanotubos de carbono de pared múltiple (MWCNT) y tetraoxomanganato (VI) de litio (LiMn$_2$O$_4$) como cátodo, usando como electrolito soporte tetrafluoroborato de litio (LiBF$_4$) disuelto en carbonato de propileno y un electrodo de referencia de Ag/AgCl. Los materiales se caracterizaron por Microscopia Electrónica de Barrido

(MEB), Análisis Termogravimétrico (ATG) y Difracción de Rayos X (DRX). Se utilizaron combinaciones de aglomerantes en los compuestos para mejorar la conductividad eléctrica en los electrodos, las propiedades mecánicas y el proceso de reversibilidad. La caracterización electroquímica reportó la existencia de dos picos anódicos y catódicos asociados al proceso de intercalación/desintercalación de los iones de litio en la interfaz electrodo/electrolito. Los resultados muestran que las combinaciones de 70%LiMn$_2$O$_4$/25%Carbón(C)/5%politetrafluoroetileno (PTFE) para el material catódico y 90% MWCNT/10%PTFE en el ánodo presentan resultados óptimos tanto para la intercalación y des intercalación del litio, y una adherencia mejorada del compuesto.

Palabras claves: Celdas de Ion-Li, LiMn$_2$O$_4$, aglomerante; voltametría cíclica, nanotubos de carbono.

INTRODUCTION

The need for the consolidation of renewable energies, owing to the depletion of fossil fuel reserves in the world, has triggered the avenue for the development of new energy storage technologies. Lithium-ion batteries are one of the alternatives for this development because they have a gravimetric energy density of approximately 150 WhKg^{-1} and are adopted as energy storage in more than 90% of portable electronic devices worldwide [1,2].

A lithium-ion battery consists of three parts, an anode, a cathode, and a conductive electrolyte. An ideal cell allows the transfer of all the ions from one electrode to the other, without suffering poisoning (transformation into subproducts), which can affect the cyclic life and energy delivery performances [3]. In these cells, the energy is stored in the electrodes in the form of lithium intercalation compounds. Commonly, graphitic materials are used as anode [4–7] and Lithium oxides as a cathode [8–10]. Beside, LiMn$_2$O$_4$, LiBOB (lithium bis-oxalate borate), and LiPF$_6$ (lithium hexafluorophosphate) are employed as an electrolyte, which is dissolved in an organic solvent, such as propylene carbonate (C$_4$H$_6$O$_3$), ethylene carbonate (C$_3$H$_4$O$_3$) or dimethyl carbonate (C$_3$H$_6$O$_3$).

In the redox process, the metal oxide is reduced, forming Li-ions that dissolve and diffuse through the electrolyte to be inserted into the anode. Neutrality is preserved by the generation of free electrons, which are transported through a cable that connects both electrodes. These free electrons promote the insertion of Li-ions into the anode [11]. The voltage on this process depends on three parameters: the metal used in the lithium oxide, the anodic material, and the electrolyte compound. During the discharge process, the reaction occurs in the opposite direction (from anode to cathode), whereas the potential difference between both electrodes produces an external current. As a result, the electrons move from anode to cathode during the discharge cycle inducing a positive current allowing the cell to act as a battery [3].

Battery improvements are conducted to optimize reversibility characteristics and increasing the gravimetric energy density. In this sense, wet cells are typically used, in which compounds and their interactions are tested by applying a potential difference. In the battery construction process, the anodic and cathodic compounds must agglomerate in the form of a paste [12]. Thus, the polymeric component and the anode or the cathode material are mixed to form a composite.

Different strategies are followed to improve the intercalation process. First, the incorporation of materials with a greater effective area. Recently, multiwall nanotubes () have been used as graphitic material in the electrodes of Li-ion batteries [13]. These carbon nanostructures show excellent mechanical properties with a high Young's modulus of approximately 1.8 TPa and flexural strength of 14.2 GPa [14]. Besides, they display high thermal conductivity from 2000-4000 WhK^{-1},

electrical conductivity about 104 Ωcm^{-1}[13]. Significantly, the MWCNTs show a high surface area of 1315 m^2g^{-1} [15–17], which is rather attractive to improve and replace the conventional graphitic material and to increase the effective area of the faradic reactions of the active particles [3,18–20]. Lee [21] reported Li-ion cells with MWCNT electrodes, which stored five times more gravimetric energy and delivering ten times more energy than a conventional Li-ion battery.

Second, the incorporation of binder materials that allow improving adherence. These materials must meet the following features: (a) being inert to electrolytes, (b) electrochemically stable in a wide potential window, and (c) they must not cause any degradation to the internal structure of the electrodes. One disadvantage of binding materials in battery fabrication is that they are electrical insulators. Typically, the concentration range of these materials lies between 5% and 10% by weight. Higher concentrations cause a significant loss in electrochemical performance. The most commonly used binding materials in the construction of electrodes are the well-known polyvinylidene fluoride (PVDF) and polytetrafluoroethylene (PTFE). The former shows drawbacks because it must be dissolved with highly toxic organic solvents such as N-methyl pyrrolidone (NMP), and N,N-dimethylacetamide (DMAC). In contrast, the PTFE dissolves in aqueous media, and consequently more friendly to health. Both display strong adhesion to metallic current collectors, which improves the chemical stability and adhesion in electrode pastes [22–25].

Herein, we used cyclic voltammetry to evaluate the electrochemical properties of wet cells built-up by using several proportions of binding compounds and incorporating MWCNTs. Thus, the combinations of different proportions of $(LiMn_2O_4)_{100\%-Z}/(Carbon)_{Z-X}/(PTFE)_X$ (where Z= 30%, X= 3%, 5%, 10%) as the

cathode and 90% MWCNT/10% PTFE as the anode were considered.

The paper is divided into several sections. Following this introduction part, the experimental methodologies are presented, which contains the methods used for the synthesis of compounds, the assembly of electrochemical measurements, and the procedures for structural characterization. The next section shows the successful preparations of products as well as its characterization through Scanning Electron Microscopy (SEM), Thermogravimetric Analysis (TGA), and powder X-ray Diffraction (PXRD) analysis. Finally, the electrochemical characterization and the results of reversibility are collected. These results showed that the 5 % PTFE lead to better performance of the built cell.

MATERIALS AND METHODS

The characterization of the morphology of the synthesized materials was conducted through a field emission scanning electron microscope (FEG-SEM) FEI Quanta 200. A Bruker D8-Focus X-ray diffractometer was used to corroborate the crystalline structure of the synthesized compounds. Thermogravimetric analysis (TGA) was done with a Mettler Toledo LF 645 TGA/DSC. The electrochemical characterization was performed through cyclic voltammetry studies with an Autolab PGSTAT302N potentiostat/galvanostat.

Synthesis of $LiMn_2O_4$

The cathode used was $LiMn_2O_4$. This metal oxide was prepared by solid-state reaction, mixing lithium carbonate (Li_2CO_3) and manganese oxide (MnO_2),following ec. 1 and with a stoichiometry ratio of 1:4. Then the mixture was sintered at 700 ºC and 800 ºC for 24 h [26,27].

$$Li_2CO_3 + 4MnO_2 \rightarrow 2LiMn_2O_4 + CO_2 + \tfrac{1}{2}O_2 \quad \text{(ec. 1)}$$
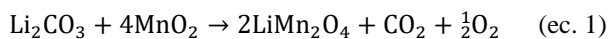
Synthesis of MWCNT

MWCNTs were used as anode material. The synthesis was conducted by chemical deposition in the vapor phase (CVD). For this, a bimetallic catalyst was introduced in 8% Fe/2% Co proportions and supported on calcium carbonate ($CaCO_3$) in a controlled chamber reaction. The reaction was carried out at 750 °C, using Ar as the carrier gas and acetylene (C_2H_2) as the carbon source (flow rate of 180 Ar/20 C_2H_2, sccm). Initially, only Ar was passed through the chamber until the temperature reached 750 °C to displace the oxygen in the chamber, and then the flow of acetylene was opened. The reaction was held for 15 minutes [28]. Subsequently, the purification of MWCNTs was carried out by refluxing with 10% hydrochloric acid (HCl), under constant stirring for 3h. Then they were filtered under vacuum and washed with abundant distilled water until reaching a neutral pH, and finally, the obtained material was dried at 120 °C during 1 h [28–33].

Electrode construction

For the preparation of the electrodes (composite material), current collector foils (with areas of 1 cm^2) of aluminum for the cathode and copper for the anode were used. The proposed compounds are formed by combinations of the cathode ($LiMn_2O_4$), graphitic carbon, and PTFE. The main objective was adding different proportions of graphite carbon to increase the conductivity of the compound and using PTFE as a binder to prevents detachment of the material during the electrochemical test. The construction procedure consisted of mixing the $LiMn_2O_4$ with graphitic carbon and PTFE in chloroform, then a reflux process was performed to agglomerate the compound and later deposited on the aluminum foil before being dried and pressed. For building the anode, a combination of

MWCNT and PTFE was used as a compound in the following proportion: 90% MWCNT/10% PTFE. Combinations that allowed to obtain a material with better adherence and to guarantee its stability during the experiments without detaching from the sheet were: 70% $LiMn_2O_4$/25% C/5% PTFE and 70% $LiMn_2O_4$/27% C/3% PTFE.

Electrochemical cell

For electrochemical characterization, one-compartment cell and three electrodes combinations described above for the cathode and anode were used. A reference electrode Ag/AgCl enclosed in an outer glass case was used and submerged in the electrolyte support (Figure 1), for which 1M $LiBF_4$ dissolved in propylene carbonate was used. The cyclic voltammetry studies were carried out in a potential window of 0.5-1.5 V *vs*. Ag/AgCl at different scan rates from 0.1 mVs^{-1} to 0.5 mVs^{-1}.
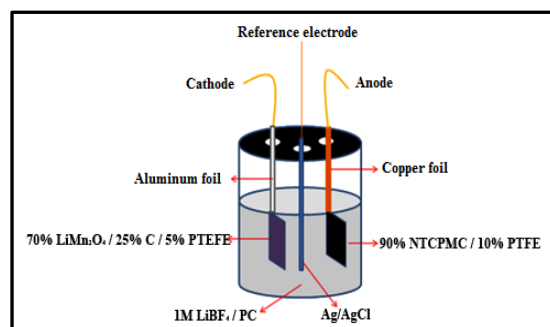

Fig. 1. Electrochemical cell diagram.

RESULTS AND DISCUSSION

Characterization of $LiMn_2O_4$

In the powder X-ray diffraction patterns (PXRD) obtained from the samples synthesized at 700 ºC and 800 ºC (Figure 2), the formation of a pure $LiMn_2O_4$ phase is observed (PDF No: 70-3120), and some phases rich in lithium ($Li_{1.4}Mn_{1.7}O_4$ PDF No: 53-821) [34], both with a cubic

crystalline structure (spinel) [35–37]. Furthermore, a shift of the diffraction maxima (Figure 2) to the right of 2θ is observed with respect to the pure phase. According to the phase diagram of the ternary system Li-Mn-O in the air [38], the stable cubic phase of $Li_{1+x}Mn_{2-x}O_4$ ($0 < x < 1/3$) is obtained in the temperature range of 700-800 ºC, the value of "x" increases with the decrease in temperature. Therefore, the lithium-rich $Li_{1.4}Mn_{1.7}O_4$ phase obtained is the product of a slow cooling rate of the sample, since as the temperature slowly decreases, manganese (Mn) and lithium (Li) continue to react, causing the value of x to increase [39–41]. For this reason, the compound cooling rate was raised for the synthesis at 700 ºC for 24 h. The PXRD analysis of the compound obtained (Figure 2) revealed the presence of a pure $LiMn_2O_4$ phase and a $Li_{0.981}Mn_{1.949}O_4$ phase (PDF No: 88-1083) [42], very close to the phase of interest, with a cubic crystalline structure (spinel) both, in the space group *Fd3m* [36,43,44], where Li-ions occupy tetrahedral sites 8*a*, manganese Mn (Mn^{3+} and Mn^{4+}) are located in octahedral sites 16*d* and those of oxygen O^{2-} are located at sites 32*e* [35,38,39,45].
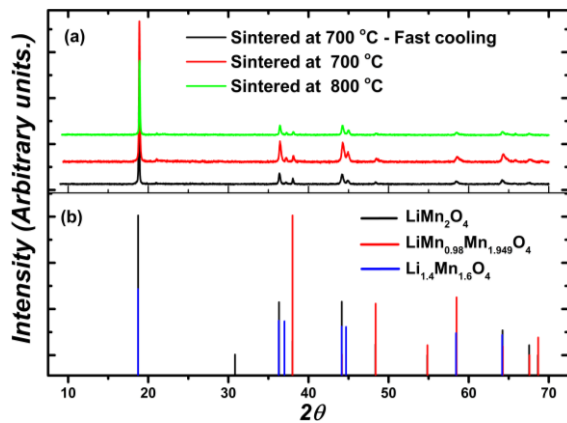

Fig. 2. Powder diffractogram (PXRD): (a). Experimental patterns at different synthesis temperatures. (b) Reference patterns of the phases $LiMn_2O_4$ (PDF No: 70-3120), $LiMn_{0.98}Mn_{1.949}O_4$ (PDF No: 88-1083) and $Li_{1.4}Mn_{1.7}O_4$ (PDF No: 53-821).

Figure 3 shows the micrographs obtained by SEM in which $LiMn_2O_4$ clusters with needle-shaped morphology can be seen [27,43]. In figure 4b a distribution of different sizes of $LiMn_2O_4$ particles is observed [27,43,45,46].
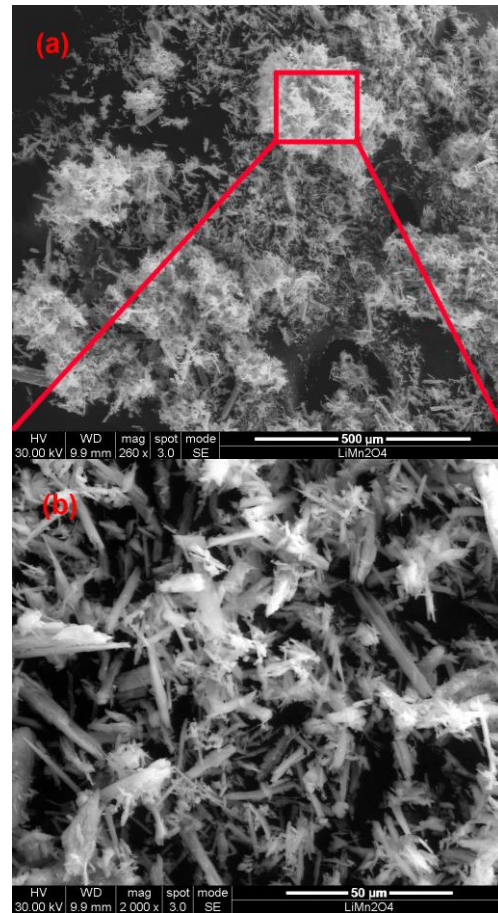

Fig. 3. Micrographs of the $LiMn_2O_4$ compound synthesized at 700 ºC for 24 h with a rapid cooling ramp, at magnifications of 250x (a) and 2000x (b).

The thermogravimetric characterization of $LiMn_2O_4$ (Figure 4), shows a mass loss of around 940 ℃ (endothermic peak in the first derivative of the decomposition curve), corresponding to the volatilization of lithium at high temperatures. The mass loss is ~6%, which indicates that the material obtained is thermally stable [46].
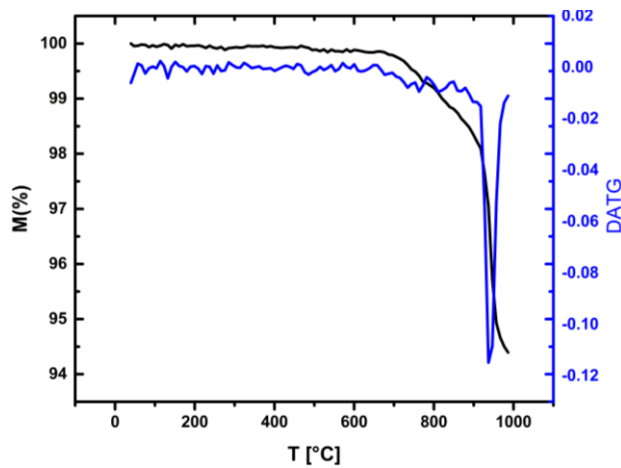
Fig. 4. Thermogram of the $LiMn_2O_4$ compound obtained at 700 ºC for 24 h with rapid cooling ramps**.**

Characterization de MWCNT

Figure 5 shows SEM images of MWCNTs after the purification procedure. Nanotubes are observed with its filiform features, cylindrical and elongated morphology with different lengths, and an average diameter of approximately ~60 nm. Figure 6a shows a powder X-rays diffraction pattern of MWCNTs, in which a corresponding maximum diffraction reflection (002) can be observed at 2θ= 26.132°. This maximum displays a displacement with respect to the reflection (002) in the graphite (Figure 6b). This could be attributed to an increase in the distance between sp^2 layers in the carbon nanotubes compared to graphite sheets. Other peaks with lower intensities are assigned to the reflections of planes (100), (101), and (004).
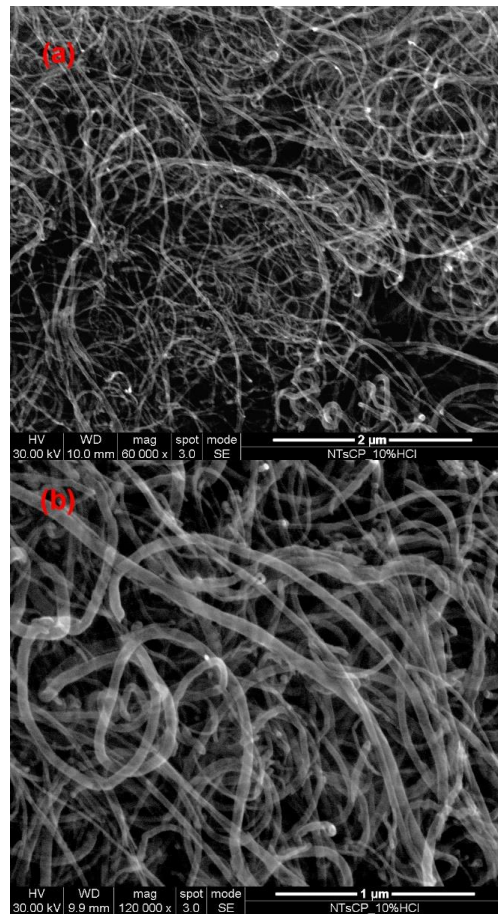

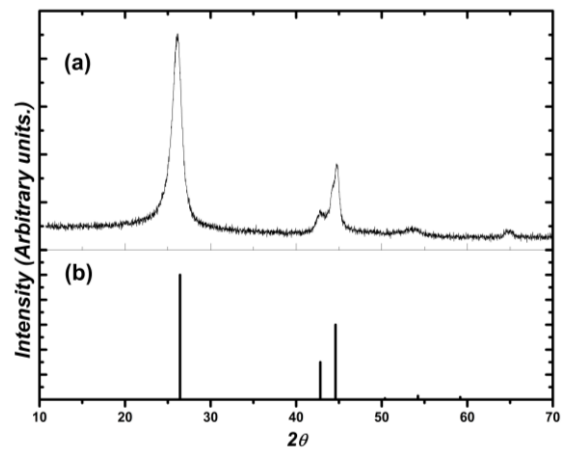**Fig. 5.** Micrographs of HCl-purified MWCNT, at magnifications of 60 kX (a) and 120 kX (b).

Fig. 6. Powder diffractogram (PXRD): (a) purified MWCNTs, (b) Reference patterns (PDF 001-0646).

Electrochemical characterization

Figure 7 shows the cyclic voltammetry carried out in cells with carbon anodes, which contain two percentages of PTFE as a binding agent in the positive electrode (70% $LiMn_2O_4$/25% C/5% PTFE and 70% $LiMn_2O_4$/27% C/3% PTFE), using a scan rate of 0.1 mVs^{-1}. In the first case (black curve), corresponding to 70% $LiMn_2O_4$/27% C/3% PTFE, oxidation waves are observed (upper black graph line) at voltages of 1.08 V and 1.21 V, and including a pair of reduction waves (lower black curve) at 0.98 V and 1.10 V. In the second case (red curve) 70% $LiMn_2O_4$/25% C/5% PTFE, oxidation waves are observed (upper red curve) at voltages of 1.07 V and 1.20 V and involving a pair of reduction waves (lower red curve) at 0.98 V and 1.12 V. In both cases, these peaks are assigned to the intercalation/deintercalation process of Li-ions at the electrode/electrolyte interface [35,47–49]. These pairs of redox peaks are associated with the occupation of two different tetrahedral sites (8*a*) in the cubic spinel structure ($LiMn_2O_4$) of lithium.

The voltammogram of Figure 7 also shows that the electrode with 3% PTFE displays higher current density compared with those that use 5% PTFE. Namely, the working electrode prepared with a lower percentage of PTFE shows a higher electrical conductivity. Strikingly, it was also observed during the voltammetric tests that the cathodic material with 3% PTFE presented the smallest detachments of material from the surface of the Al sheet. These results suggest that 5% of PTFE material is a suitable composition for voltammetry studies of an electrode containing MWCNTs as an anode.
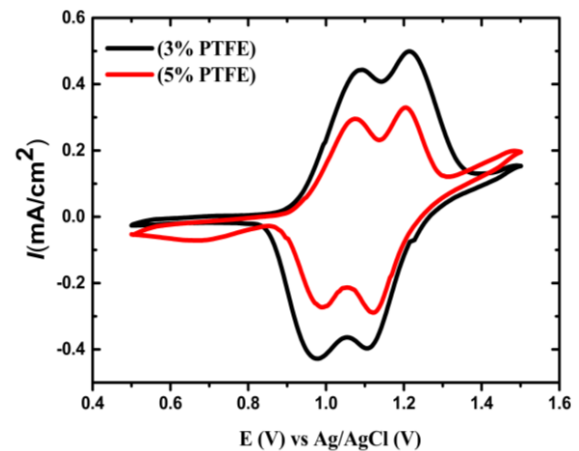

Fig. 7. Cyclic voltammetry in wet cells with carbon anode. (*v*= 0.1 mVs^{-1}).

Figure 8 shows the cyclic voltammetry of the electrochemical cell when 70% $LiMn_2O_4$/25% C/5% (PTFE) compound was used as the cathode, the 90% MWCNT/10% PTFE compound as the anode, and the Ag/AgCl as the reference electrode, in a potential window of 0.5 V to 1.5 V *vs*. Ag/AgCl, at a scan rate of 0.1 mVs^{-1}. In the direct scan, a pair of oxidation waves can be observed (upper of the graph) at 1.07 V and 1.21 V, and in the reverse direction, two reduction waves (lower of the graph) at 1.01 V and 1.14 V. These waves are attributed to the Li-ion intercalation/deintercalation processes. The two pairs of redox waves observed are attributed to lithium occupation of two different tetrahedral sites 8*a* in the cubic structure of $LiMn_2O_4$. The first of these waves is assigned to the deintercalation of Li-ion from the tetrahedral sites, where exists Li-Li interactions, and the second to the deintercalation of Li-ion from the tetrahedral sites where Li-Li interactions do not occur. The two waves in the reverse direction agree to the Li-ions intercalation process at the 16*c* octahedral sites of the cubic structure, thus causing a first-order transition from a cubic to a tetragonal structure [50].
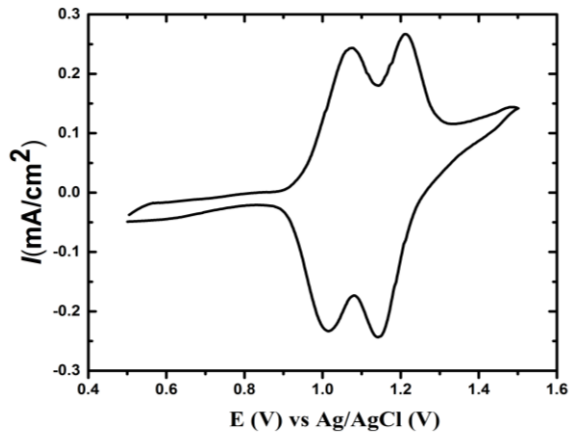
Fig. 8. Cyclic voltammetry of 70 % LiMn$_2$O$_4$, 25 % C y 5 % PTFE, in LiBF$_4$ 1M (ν = 0.1 mVs^{-1})

Fig. 9. Li-ion cell scan rate study; cathode: 70% LiMn$_2$O$_4$, 2% C and 5% PTFE, anode: 90% MWCNT / 10% PTFE, in 1M LiBF$_4$.

Figure 9 shows the scan rate study for the Li-ion cell containing MWCNTs in the anode. This figure shows the existence of two pairs of well-defined redox waves for the different scan rates, related to the Li-ion intercalation/deintercalation processes in the electrode/electrolyte interface [44,51,52]. The figure displays a clear separation of both the anodic and cathodic peaks. The Nicholson and Shain criteria for reversible processes were used to evaluate the reversibility of the system [53,54]:

1) $\Delta E_p = \Delta E_{pA} - \Delta E_{pC} = \frac{59}{n} mV$
2) $|E_p - E_{\frac{p}{2}}| = \frac{59}{n} mV$
3) $\left|\frac{I_{PA}}{I_{pC}}\right| = 1$
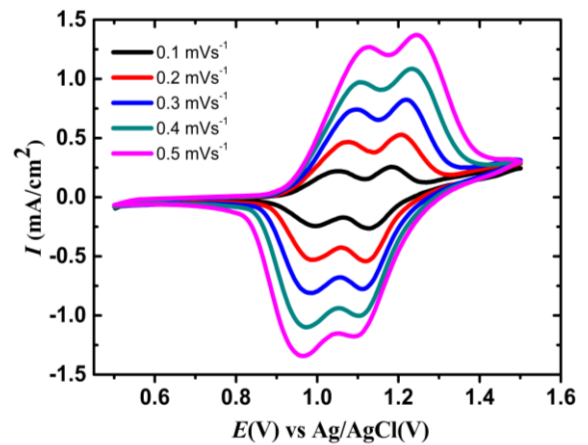4) $I_p \propto \nu^{1/2}$
5) E_p is independent from ν

Table 1 register the electrochemical parameter values calculated from the cyclic voltammetry at different scan rate for the 70% LiMn$_2$O$_4$/ 25% C/5% PTFE cell, anode: 90% MWCNT/10% PTFE, in 1M LiBF$_4$.

Table 1**. -** Electrochemical parameters calculated from Figure 9

ν (mVs^{-1})	ΔE_{p1} (mV)	I_{pa1}/I_{pc1}	ΔE_{p2} (mV)	I_{pa2}/I_{pc2}
0.1	58.6	0.90	61.0	0.98
0.2	87.9	0.88	90.3	0.97
0.3	122.3	0.99	109.8	1.06
0.4	131.8	0.88	131.8	1.08
0.5	165.5	0.94	156.2	1.16

In Table 1, separations of anodic and cathodic peaks observed from the evaluation of the criterium 1, can be attributed to the thickness of the prepared film. For significant thicknesses (> 2mm), the potentials on the electrodes cannot be uniform or homogeneous, inducing a limitation for the Li-ions diffusion from the surface to the center of the electrode [55]. Thus, a thickness exceeding of the electrode may produce a drop of potential [56].

Figure 10 presents the evaluation of the criterium 4, whereby the density current must be proportional to the square root of the scan rate, showing a straight line that

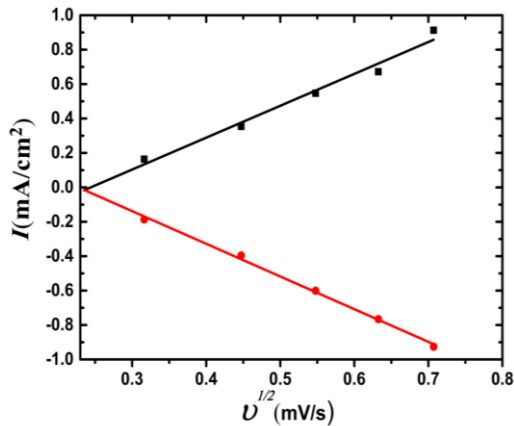confirms the proportionality and that the process is controlled by the diffusion of Li-ion in the sample.

Fig. 10. Graph of I_p vs $\nu^{1/2}$.

The evaluation of Nicholson and Shain's criterium number 5 is shown in Figure 11, where it is observed that as the scan rate increases, the oxidation and reduction peaks potentials shift to more positive and negative values, respectively. This behavior is attributed to a sharp potential drop or to increased resistance of the electrode due to a slow electron transfer [57–59].
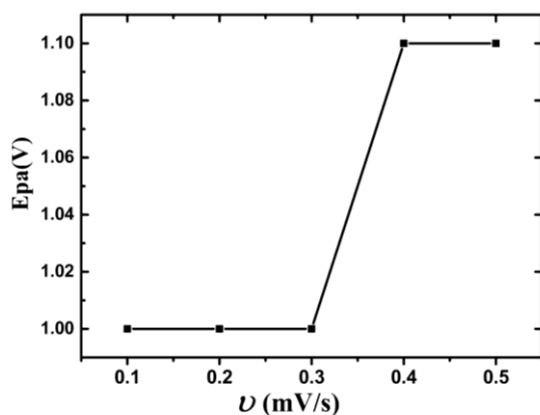

Fig. 11. Graph of E_p vs ν.

CONCLUSION

Our studies presented the analysis of different proportions of binders in Li-ion cells using MWCNTs in the anode and

$LiMn_2O_4$ as the cathode. Both compounds were fully synthesized and characterized. The use of these compounds in the construction of electrochemical cells is related to the development of mixtures that meet two main features: (a) achieving improved mechanical properties that allow superior stability of the compound during electrochemical evaluation and (b) maximizing electrical conductivity. Reaching this compromise between both characteristics is a technological challenge since the best binders are non-conductive polymeric materials that coat the active sites, impairing the transmission of electrons. Our study shows that even though the use of the 70% $LiMn_2O_4$/27% C/3% PTFE compound presented a slightly higher current density than the $LiMn_2O_4$/27% C/5% PTFE compound, the first compound detached from the collector plate during the voltammetric study, so we conclude that the second compound with 5% PTFE is a better candidate. When evaluating the reversibility criteria based on Nicholson and Chain, we found that the system is quasi-reversible, since the peak potentials vary respect to the scan rate. At speeds higher than 0.4 mVs^{-1}, the ΔEp increases with increasing speed. This is attributable to the thickness of the plates. In the case of the wet cells, this thickness must be kept between 1-2 mm to guarantee the stability of the compound, but in the dry cells, it must be decreased, which should improve the reversibility of the system. The characterization of the dry cell of the compounds presented in this study will be the subject of discussion for future work.

REFERENCES

[1]. Arora P., Zhang Z. (2004). "Battery separators". *Chem. Rev.* 104(10):4419–62

[2]. Manthiram A. (2020). "A reflection on lithium-ion battery cathode chemistry". *Nat. Commun.* 11(1):1–9

[3]. Sehrawat P., Julien C., Islam S.S. (2016).

"Carbon nanotubes in Li-ion batteries: A review". *Mater. Sci. Eng. B*. 213:12–40

[4].   Shimoda H., Gao B., Tang X., Kleinhammes A., Fleming L., Wu Y., Zhou O. (2001). "Lithium Intercalation into Opened Single-Wall Carbon Nanotubes: Storage Capacity and Electronic Properties". *Phys. Rev. Lett.* 88(1):015502-1/015502-4

[5].   Wu Y.P., Rahm E., Holze R. (2003). "Carbon anode materials for lithium ion batteries". *J. Power Sources*. 114(2):228–36

[6].   Wang H., Dai Q., Li Q., Yang J., Zhong X., Huang Y., Zhang A., Yan Z. (2009). "Preparation of porous carbon spheres from porous starch". *Solid State Ion.* 180(26–27):1429–32

[7].   Martínez I.C. (2011). "Preparación De Materiales Grafíticos: aplicación como ánodos en baterías de ion-litio". Universidad de oviedo, Departamento de Química Orgánica e Inorgánica

[8].   Lee Y.S., Sun Y.K., Nahm K.S. (1998). "Synthesis of spinel $LiMn_2O_4$ cathode material prepared by an adipic acid-assisted sol-gel method for lithium secondary batteries". *Solid State Ion.* 109(3–4):285–94

[9].   Kosova N. V., Uvarov N.F., Devyatkina E.T., Avvakumov E.G. (2000). "Mechanochemical synthesis of $LiMn_2O_4$ cathode material for lithium batteries". *Solid State Ion.* 135(1–4):107–14

[10].   Liu Z., Yu A., Lee J.Y. (1998). "Cycle life improvement of $LiMn_2O_4$ cathode in rechargeable lithium batteries". *J. Power Sources*. 74(2):228–33

[11].   Linden D., Reddy T.B. (2004). "*Handbook of batteries*". New York: McGraw-Hill. pp. 1.3-1.18

[12].   Besenhard J.O., Daniel C. (1999). "*Handbook of battery material*". Weinheim: WILEY-VCH Verlag. pp. 19–58

[13].   Morris R.S., Dixon B.G., Gennett T., Raffaelle R., Heben M.J. (2004). "High-energy , rechargeable Li-ion battery based on carbon nanotube technology". *J. Power Sources 138*. 138:277–80

[14].   Lv J., Tu J.P., Zhang W.K., Wu J.B., Wu H.M., Zhang B. (2004). "Effects of carbon nanotubes on the high-rate discharge properties of nickel/metal hydride batteries". *J. Power Sources*. 132(1–2):282–87

[15].   Peigney a., Laurent C., Flahaut E., Bacsa R.R., Rousset a. (2001). "Specific surface area of carbon nanotubes and bundles of carbon nanotubes". *Carbon*. 39(4):507–14

[16].   Thostenson E.T., Ren Z., Chou T. (2001). "Advances in the science and technology of carbon nanotubes and their composites : a review". *Compos. Sci. Technol.* 61:1899–1912

[17].   Belin T., Epron F. (2005). "Characterization methods of carbon nanotubes: a review". *Mater. Sci. Eng. B*. 119(2):105–18

[18].   De Las Casas C., Li W. (2012). "A review of application of carbon nanotubes for lithium ion battery anode material". *J. Power Sources*. 208:74–85

[19].   Xiong Z., Yun Y., Jin H.-J. (2013). "Applications of Carbon Nanotubes for Lithium Ion Battery Anodes". *Materials*. 6(3):1138–58

[20].   Ng S.H., Wang J., Guo Z.P., Chen J., Wang G.X., Liu H.K. (2005). "Single wall carbon nanotube paper as anode for lithium-ion battery". *Electrochim. Acta*. 51(1):23–28

[21].   Lee S.W., Yabuuchi N., Gallant B.M., Chen S., Kim B.-S., Hammond P.T., Shao-Horn Y. (2010). "High-power lithium batteries from functionalized carbon-nanotube electrodes.". *Nat. Nanotechnol.* 5(7):531–37

[22].   Zhu Z., Tang S., Yuan J., Qin X., Deng Y., Qu

R., Haarberg G.M. (2016). "Effects of various binders on supercapacitor performances". *Int. J. Electrochem. Sci.* 11(10):8270–79

[23]. Priyono S., Lubis B.M., Humaidi S., Prihandoko B. (2018). "Heating Effect on Manufacturing $Li_4Ti_5O_{12}$ Electrode Sheet with PTFE Binder on Battery Cell Performance". *IOP Conf. Ser. Mater. Sci. Eng.* 367(1):0–6

[24]. Shi Y., Zhou X., Yu G. (2017). "Material and Structural Design of Novel Binder Systems for High-Energy, High-Power Lithium-Ion Batteries". *Acc. Chem. Res.* 50(11):2642–52

[25]. Song B., Wu F., Zhu Y., Hou Z., Moon K. sik., Wong C.P. (2018). "Effect of polymer binders on graphene-based free-standing electrodes for supercapacitors". *Electrochim. Acta*. 267:213–21

[26]. Zhang S.S., Jow T.R. (2002). "Optimization of synthesis condition and electrode fabrication for spinel $LiMn_2O_4$ cathode". *J. Power Sources*. 109:172–77

[27]. Chen Z., Huang K., Liu S., Wang H. (2010). "Preparation and characterization of spinel $LiMn_2O_4$ nanorods as lithium-ion battery cathodes". *Trans. Nonferrous Met. Soc. China*. 20(12):2309–13

[28]. Bronikowski M.J. (2006). "CVD growth of carbon nanotube bundle arrays". *Carbon*. 44(13):2822–32

[29]. Guan B.H., Ramli I., Yahya N., Pah L.K. (2011). "Purification of Carbon Nanotubes Synthesized by Catalytic Decomposition of Methane using Bimetallic Fe-Co Catalysts Supported on MgO". *IOP Conf. Ser. Mater. Sci. Eng.* 17 012025:1–5

[30]. Paradise M., Goswami T. (2007). "Carbon nanotubes – Production and industrial applications". *Mater. Des.* 28(5):1477–89

[31]. Xuan T.T. (2011). *Croissance catalytique et etude de nanotubes de carbone multi-feuillets produits en masse et de nanotubes de carbone ultra-long individuels a quelques feuillets*. Universite montpellier II, Institute of Materials Science

[32]. Sampedro-Tejedor P., Maroto-Valiente A., Nevskaia D.M., Múñoz V., Rodríguez-Ramos I., Guerrero-Ruíz A. (2007). "The effect of growth temperature and iron precursor on the synthesis of high purity carbon nanotubes". *Diam. Relat. Mater.* 16(3):542–49

[33]. Hernández V., J. Arévalo., Plaza E., Diaz L., Sosa E., Morales R., Atencio R. (2013). "Purification of MWCNT and its characterization by scanning electron microscopy and thermogravimetric analysis". *Acta Microsc.* 22(3):256–61

[34]. Dudney, N., Bates, J., Zuhr, R., Young, S., Robertson, J., Jun, H., Hackney S. (1999). "Nanocrystalline $Li_xMn_{2-y}O_4$ Cathodes for Solid-State Thin-Film Rechargeable". *J. Electrochem. Soc.* 146(7):2455–64

[35]. Park S., Okada S., Yamaki J. (2011). "Symmetric Cell with $LiMn_2O_4$ for Aqueous Lithium-ion Battery". *J. Nov. Carbon Resour. Sci.* 3:27–31

[36]. Cha-quing X., Yan-wen T., Yu-chun Z., Bing Y., Zhao-jing G. (2004). "Synthesis and character of spinel $LiMn_2O_4$". *trans. Nonferrous Met. Soc. China*. 14(3):470–74

[37]. He X., Wang L., Pu W., Zhang G., Jiang C., Wan C. (2006). "Synthesis of Spinel $LiMn_2O_4$ for Li-Ion Batteries via Sol-gel Process". *Int. J. Electrochem. Sci.* 1:12–16

[38]. Luo C. (2005). "Investigation on the Phase Stability and Defect Structure of Li-Mn-O and Li-Me-Mn-O Spinel (Me = Mg , Ni , Co)". Rwth aachen university, Fakultät für Mathematik, Informatik und Naturwissenschaf

[39]. Paulsen J.M., Dahn J.R. (1999). "Phase Diagram

of Li - Mn - O Spinel in Air". *Chem. Mater.* 4:3065–79

[40]. Eriksson T. (2001). "LiMn$_2$O$_4$ as a Li-Ion Battery Cathode". Universitets Uppsala, Faculty of Science and Technology

[41]. Yonemura M., Yamada A., Kobayashi H., Tabuchi M., Kamiyama T., Kawamoto Y., Kanno R. (2004). "Synthesis, structure, and phase relationship in lithium manganese oxide spinel". *J. Mater. Che m.* 14:1948–58

[42]. Ishikawa, Y., Higuchi S. (1997). "Structure analysis of some Li-metal double oxides". *Toso Kenkyu Hokoku.* 41:35–41

[43]. Kim D.K., Muralidharan P., Lee H.-W., Ruffo R., Yang Y., Chan C.K., Peng H., Huggins R. a., Cui Y. (2008). "Spinel LiMn$_2$O$_4$ nanorods as lithium ion battery cathodes.". *Nano Lett.* 8(11):3948–52

[44]. Kiani M.A., Mousavi M.F., Rahmanifar M.S. (2011). "Synthesis of Nano- and Micro-Particles of LiMn$_2$O$_4$: Electrochemical Investigation and Assessment as a Cathode in Li Battery". *Int. J. Electrochem. Sci.* 6:2581–95

[45]. Yi T.-F., Hao C.-L., Yue C.-B., Zhu R.-S., Shu J. (2009). "A literature review and test: Structure and physicochemical properties of spinel LiMn$_2$O$_4$ synthesized by different temperatures for lithium ion battery". *Synth. Met.* 159(13):1255–60

[46]. Wu H.M., Tu J.P., Yuan Y.F., Chen X.T., Xiang J.Y., Zhao X.B., Cao G.S. (2006). "One-step synthesis LiMn$_2$O$_4$ cathode by a hydrothermal method". *J. Power Sources.* 161(2):1260–63

[47]. Huang Y., Li J., Jia D. (2005). "Preparation and characterization of LiMn$_2$O$_4$ nanorod by low heating solid state coordination method". *J. Nanoparticle Res.* 6(1):533–38

[48]. Singhal R., Das S.R., Tomar M.S., Ovideo O.,

Nieto S., Melgarejo R.E., Katiyar R.S. (2007). "Synthesis and characterization of Nd doped LiMn$_2$O$_4$ cathode for Li-ion rechargeable batteries". *J. Power Sources.* 164(2):857–61

[49]. Zhang Y., Shin H.C., Dong J., Liu M. (2004). "Nanostructured LiMn$_2$O$_4$ prepared by a glycine-nitrate process for lithium-ion batteries". *Solid State Ion.* 171(1–2):25–31

[50]. Christiansen T.L., Bojesen E.D., Sondergaard M., Birgisson S., Becker J., Iversen B.B. (2016). "Crystal structure, microstructure and electrochemical properties of hydrothermally synthesised LiMn2O4". *CrystEngComm.* 18(11):1996–2004

[51]. Bai Y., Wu C., Wu F., Wang G. (2006). "Cyclic voltammetry studies on 4 V and 5 V plateaus of non-stoichiometric spinel Li$_{1+x}$Mn$_{2-y}$O$_4$". *Trans. Nonferrous Met. SOC. China.* 16(2):402–8

[52]. Xian-ming W.U., Zhuo-bing X., Ze-qiang H.E., Xin-hai L., Shang C., Engineering C., Science M. (2006). "Characterization of rapid thermally processed LiMn$_2$O$_4$ thin films derived from solution deposition". *trans. Nonferrous Met. Soc. China.* 16(3):545–50

[53]. Nicholson R.S., Shain I. (1964). "Theory of Stationary Electrode Polarography: Single Scan and Cyclic Methods Applied to Reversible, Irreversible, and Kinetic Systems". *Anal. Chem.* 36(4):706–23

[54]. Matsuda H., Ayabe Y. (1955). "Zur Theorie der Randles-Sevčikschen Kathodenstrahl-Polarographie". *Zeitschrift fuer Elektrochemie.* 54(6):494–503

[55]. Tsay K.C., Zhang L., Zhang J. (2012). "Effects of electrode layer composition/thickness and electrolyte concentration on both specific capacitance and energy density of supercapacitor". *Electrochim. Acta.* 60:428–36

[56].   Lindstrom Henrik., So S., Solbrand A., Hjelm J.,
        Hagfeldt A., Lindquist S. (1997). "Li Ion
        Insertion in TiO_2(Anatase), Voltammetry on
        Nanoporous Films". *J. Phys. Chem. B*.
        2(97):7717–22

[57].   Lim M., Cho W., Kim K. (2001). "Preparation
        and characterization of gold-codeposited
        $LiMn_2O_4$ electrodes". *J. Power Sources*. 92:168–
        92

[58].   Takahashi M., Tobishima S. ichi., Takei K.,
        Sakurai Y. (2002). "Reaction behavior of
        LiFePO4 as a cathode material for rechargeable
        lithium batteries". *Solid State Ion.* 148(3–4):283–
        89

[59].   Kim T., Choi W., Shin H.C., Choi J.Y., Kim
        J.M., Park M.S., Yoon W.S. (2020).
        "Applications of voltammetry in lithium ion
        battery research". *J. Electrochem. Sci. Technol.*
        11(1):14–25